Adaptive Fuzzy and Predictive Controllers for Expressive Robot Arm Movement during Human and Environment Interaction

Liz Rincon Ardila, Enrique Coronado, Hansen Hendra, Julyando Phan, Zur Zainalkefli, Gentiane Venture
Tokyo University of Agriculture and Technology 2-21-16 Nakacho, Koganei, Tokyo, Japan
Email: lizrincon@m2.tuat.ac.jp

***Abstract*—To create robots able to generate expressive motions and improve human robot interaction (HRI). An innovative adaptive control system architecture for a robot arm is developed which can adapt the control parameters and motion trajectories according to the perception generated by the human, the environment, and the overall robot interaction. An adaptive fuzzy controller that maps environmental and HRI factors to the PAD emotional model (Pleasure, Arousal, and Dominance) is proposed. These PAD values are used to change the robot strategy to generate trajectories and control parameters, which are designed to express different emotional states. The robot motions are commanded by the Robust Generalized Predictive Controllers (RGPC), using optimization by Youla parameters, that involves robot regulation with adaptive motion. The optimization control uses an adaptive receding horizon designed according to the response of the human and environment interaction. This proposal allows to generate motions with more personalized characteristics for human robot interaction in a non-humanoid robots.**

***Index Terms*—robot arm, adaptive fuzzy control, adaptive robust predictive control, affective robotics**

I. Introduction

Robots with the ability to cooperate with people and interact in social contexts are now being used in diverse scenarios. To enable long-term interactions, these robots must be able to convey a sense of believability, diversity and adaptation to environmental conditions [1]. It is often said that a key factor in creating intelligent social agents is the ability to express different affective states [2]. However, even when a large portion of human-human affective communication is expressed with gestures and postures [3], most studies related to emotional expression in robotics focused in artificially reproduced human-like facial expressions. Two notable examples are [4] and [5]. Moreover, many robots available on the market cannot perform facial expression due to the mechanical or technological limitations. Examples of these types of robots are mobile robots, manipulator robots, and quadropters, among others. Literature in affective computing reports very few works addressing the challenges that imply the use of non-zoomorphic robots, and even fewer when they have no face [6], [7]. Furthermore, studies that use arm-robots to express emotions are still very rare.

In this work, an interactive robot arm able to generate representative expressive states (postures/motions) while taking into account environmental factors and human interaction is created. For this, a new architecture is proposed where predictive controllers are designed and implemented to produce robot motion with expressive trajectories and postures, and the new adaptive receding horizon involving the human and environmental states is designed to execute the control optimization. We also propose a high-level, adaptive, fuzzy-based system that infers the internal emotion of the robot from both environmental conditions and human actions. The fuzzy system outputs are used as inputs of the low-level predictive controller to generate dynamic and personalized behaviors.

This paper is organized as follows. In Section II, related works and contributions are discussed. Section III describes the robot control architecture. Section IV develops the adaptive fuzzy controller. Section V presents the design of the robust predictive controller. Section VI describe the simulation results, Section VII presents the experimental and evaluation results. Finally, the conclusions are presented.

II. Related Works and Contributions

Emotions and mood are important elements in affective computing. While emotions are generally expressed using instantaneous behaviors, such as facial expressions or gestures, moods are longer-lived and affect human behaviors [8]. A well-known model used in affective computing for encoding both emotions and moods is the PAD (Pleasure-Arousal-Dominance) dimensional model [9], [10]. In this 3D model, general mood types are divided in eight octants, and emotional states are represented as moving vectors with the current pleasure, arousal and dominance values. The *pleasure* component of the PAD model represents an affective balance and varies from positive to negative. The *arousal* component indicates the degree of physical activity and varies from excited to calm. Finally, the *dominance* component represents the degree of control or influence

Manuscript received March 28, 2018; revised February 4, 2019.

doi: 10.18178/ijmerr.8.2.207-219

over the environment and varies from weak to strong [11]. Fig. 1 shows how some emotional states are mapped in the PAD model.

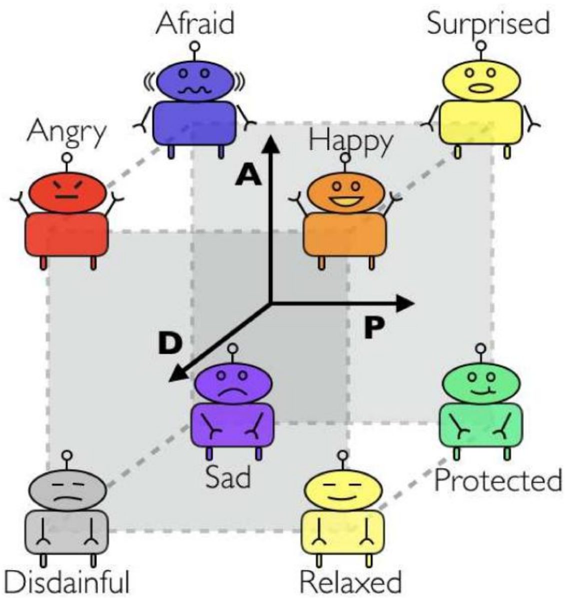

Figure 1. PAD emotional model [10]

The PAD model has been widely used in studies on virtual agents and computer gaming [12], [13] as well as robotics. A relevant example is described in [14], where the PAD model is mapped in motion features (jerkiness, activity and gaze) to generate affective movement of an anthropomorphic robot. Another approach is shown in [15], where the PAD model and fuzzy logic were applied in a humanoid robot to simulate internal emotional states and reach emotional coherence over time.

Different controllers were proposed to enhance the robot arms' performance [16], [17] in executing specific tasks. The predictive controllers are used extensively for other systems in industrial applications, but rarely for these kinds of expressive robots. Some other robot controllers [18], [19] were developed with focus on incremental precision during the tracking trajectory for manipulation tasks. However, using these controllers with robot arms to express motions with sensations according to the human interaction in a social context and relate to the environmental changes, is not widely developed.

Our focus differs in the use of a non-humanoid robot, in this case a robot arm. Additionally, environmental conditions, such as temperature, humidity, and brightness as factors that affects the robot's emotional states are considered. Even when these environmental variables are considered important moderators of emotional states [20], they are generally ignored in affective computing studies for human robot interaction.

The proposed emotional system also uses the robot's internal state (the robot temperature) and some social states of the human face (smiles and human engagement) to adapt the values of the membership functions in the proposed fuzzy-based model. Moreover, the design of robust predictive controllers for regulation and motion generation that produce the expressive states of a robot arm is also presented.

The contributions of this paper are focused on creating expressive states for robots, taking into account the interaction not only of the human but also of the environment and the robot's internal states, and creating a direct relation with the design of the adaptive controllers and motion generation. The contributions can be listed as follows:

I. Development of an adaptive architecture based on the robotic framework using NEP (Node Primitives).

II. Proposal of an Adaptive Fuzzy Inference System to represent perception and decision-making in cognitive controllers based on the emotional model PAD. The PAD is created with the human environment interaction and robot internal states. These inputs and adaptive parameters directly affect the standard deviation of the fuzzy membership functions, moving the final PAD to generate the robot's expressive motions.

III. Implementation of predictive controllers designed with an adaptive prediction horizon. The final prediction horizon is adapted according to the PAD information (human and environment). It is used to optimize the cost function and predict the robot's control output signal.

IV. Development of the control functions in the PAD and mapping calculation to personalize the robot arm's expressive motions.

III. Robot Control System Architecture

The system architecture developed is shown in Fig. 2. This modular architecture is composed of different levels to understand the robot's interactions with the environment and the human. It converts these inputs into suitable actions for generating the representative states in the robot. The architecture has a perception level that combines the environment, the human, and the robot states. The other level is the robot cognition, which involves the fuzzy emotional system and the decision-making process to create the strategic motion. Finally, in the architecture, the robot control system involves the predictive controllers to regulate and keep the motion trajectory in accordance with the adaptability of the perception states.

In the perception level, three components are considered: environment, human, and robot states. The first component, denoted as *environmental state component*, reads the data via serial port provided by a microcontroller board STM32F446 Nucleo-64. This microcontroller processes the signals of some sensors which monitor environmental conditions (temperature, humidity and brightness for example). The temperature sensor works with a temperature range, 0–100 ℃, with a linear analogical output 10 mV/℃, and error < 1.5 mV. The humidity sensor has a range of 20–80% with ±5% of variation. The brightness is measured with a photo-resistor that changes according to light intensity. Additional sensors can be added at will, to extend the capabilities and acquire more information of the environment and human interaction.

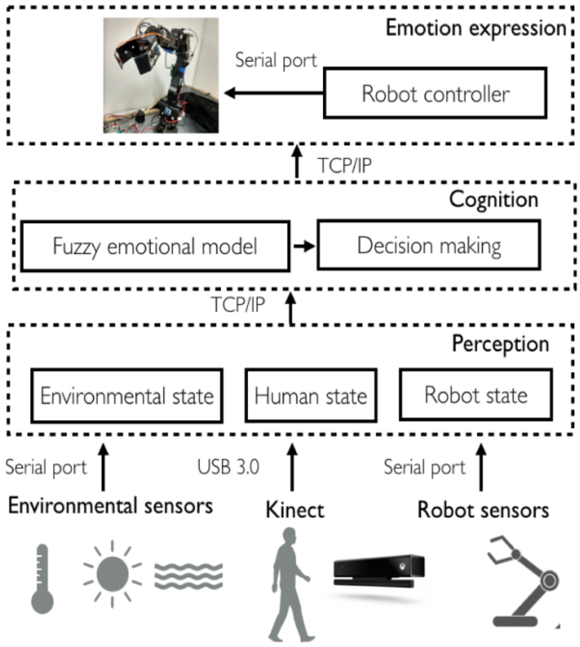

Figure 2. System architecture used for simulation and expression of robot states

The second perceptual component, denoted as the *human state component*, reads the state of the interaction between a human and the robot. For this, an interface is developed based on C\# and the Microsoft Kinect Software development Kit to process the data obtained from a Microsoft Kinect V2. This kind of motion capture device, initially conceived for home gaming, is now widely used for human action recognition in biomechanical and robotic research [21]. This device can create a depth map and detect several human joints in the range of 0.5 to 8 m. These capabilities are used to estimate the distance between the human and the robot. Also, the device's face recognition capabilities are applied to detect actions that can influence the robot's emotional states, such as a human smile and direction of gaze.

The last perceptual component is the *robot state component*, and it is used to get the current internal states that can affect the robot's emotions or comfort. For the robot perception input, the motor's average temperature is taken into account. This perceptual data is published to the local network for posterior processing.

The architecture's cognition level is based on Python modules; it is applied to perform the high-level emotional modeling using information from the perceptual components. This modeling uses an adaptive fuzzy logic controller to get the robot's current PAD value in function of the perceptual inputs and k-nearest neighbors to classify emotion (detailed in section IV). It generates the robot's current emotional state. This component publishes two outputs to the local network. The first is a string indicating the current emotional state, which is used to select the trajectories performed by the robot. The second is the current value of the robot's PAD model. This output is used to modify the motion parameters in the controller.

Finally, the robot state expression level generates the control actions and the expressive motions through robust predictive controllers (RGPC), which use convex optimization to calculate the polynomials for regulating the dynamic of the emotional trajectory and the internal feedback for the robot motion. These controllers are based on GPC stable controllers, which are designed with an adaptive term (final predictive horizon) to execute the optimization. The final horizon is determined based on the human and environment interaction modeled by the PAD in the fuzzy system. The RGPCs are programmed in MATLAB and communicate with the other modules via TCP/IP.

The NEP (Node Primitives) robotic framework is configured to communicate all the different components written in different programming languages by the publish-subscriber and client-server communication patterns [22]. This framework, proposed in [23], was developed to be easy to install, compatible with Robot Operating System (ROS) [24], human-centered and cross-platform. In this work, a non-anthropomorphic robot arm with 5-DoF is used to express emotional states with the NEP robotic framework.

An advantage of this architecture is the modularity of the proposed system architecture that makes practical the execution of the developed algorithms in any robot platform.

The robot arm used for this work was previously identified using the inertial parameters identification of the standard base, and dynamic and geometrical identification of the end-effector. The modeling values are specified in [25].

The robot identification is implemented to determine the dynamic model related to the inertia matrix, Coriolis, gravitational and friction torque effects are shown in (1). The robust predictive controllers are designed according to the robot dynamic model, characterized by each joint motion.

$$\begin{gathered}\boldsymbol{\Gamma} = \mathbf{M}(\boldsymbol{\theta})\ddot{\boldsymbol{\theta}} + \mathbf{C}(\boldsymbol{\theta},\dot{\boldsymbol{\theta}})\dot{\boldsymbol{\theta}} + \mathbf{G}(\boldsymbol{\theta}) + \boldsymbol{\Gamma}_{\boldsymbol{f}} \\ \boldsymbol{\Gamma}_{\boldsymbol{f}} = diag(\ddot{\boldsymbol{\theta}})\mathbf{F}_v + diag\left(sign(\ddot{\boldsymbol{\theta}})\right)\mathbf{F}_c\end{gathered} \tag{1}$$

Where $\boldsymbol{\theta}$, $\dot{\boldsymbol{\theta}}$ and $\ddot{\boldsymbol{\theta}}$ are the $(N_J \times 1)$ vectors of joint angles, velocities and accelerations, $\mathbf{M}(\boldsymbol{\theta})$ $(N_J \times N_J)$ is the robot inertia matrix, $\mathbf{C}(\boldsymbol{\theta}, \dot{\boldsymbol{\theta}})$ $(N_J \times 1)$ are the Coriolis and centrifugal terms, and $\mathbf{G}(\boldsymbol{\theta})$ $(N_J \times 1)$ is the gravitational term. $\mathbf{F}_f(N_J \times 1)$ is the vector of friction torques due to $\mathbf{F}_c$ Coulomb and $\mathbf{F}_v$ Viscous friction effects.

IV. Adaptive Fuzzy Logic Controller

In natural conversation, affective states are always defined with linguistic variables. In fact, one often says things like: "*you are very happy*" or "*he seems a little bit sad*." Moreover, these linguistic variables have

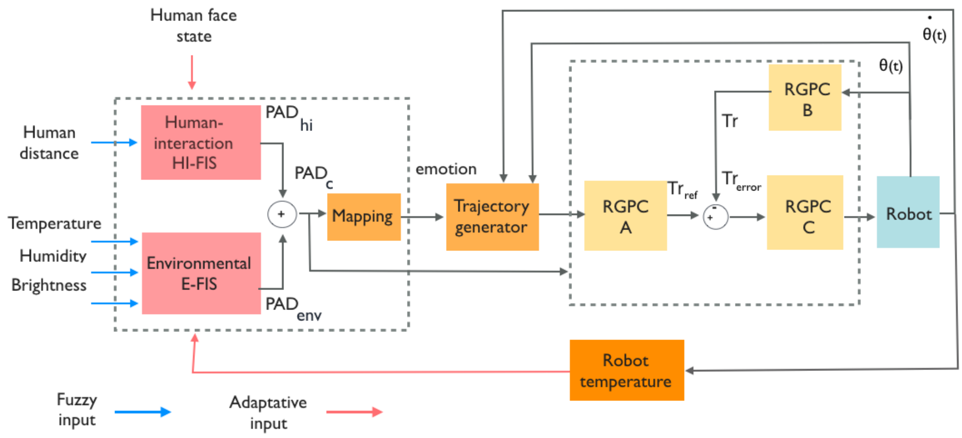

Figure 3. Control Architecture proposal for expression of emotional states in robot arm

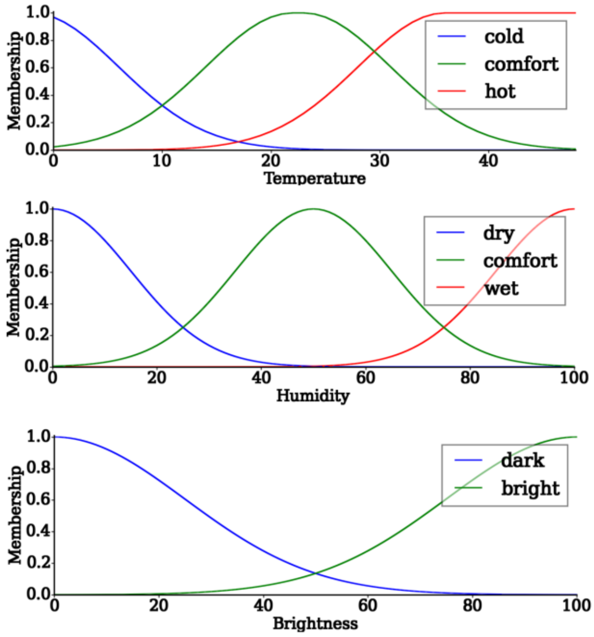

Figure 4. Environment parameters: modeling in the Environmental -Fuzzy Inference System (EFIS) inputs definitions

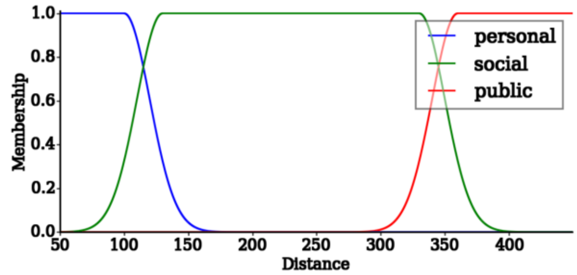

Figure 5. Human proximity membership functions for the Human-Interaction Fuzzy Inference System (HI-FIS)

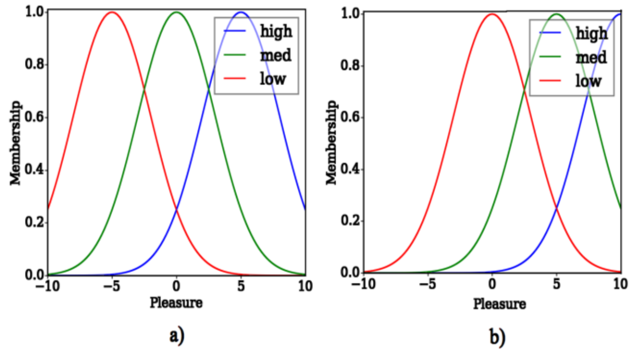

Figure 6. a) Pleasure PAD-output without adaptive input, b) Pleasure PAD-output with positive adaptive input

unclear boundaries between them and can vary depending on the human personality, the environment, or the context. A powerful approach that can be used to model this uncertainty is the fuzzy logic [26]. The advantage of this technique is that the solution of a problem can be defined in terms of unclear linguistic variables. Therefore, human experience can be modeled easily.

Fig. 3 shows the proposed Adaptive Fuzzy Emotional Model (AFEM) scheme. This approach is composed of two Fuzzy Inference Systems (FIS). These blocks model the environmental conditions and human activities' influence on the robot's affective states. These blocks are Environmental Fuzzy Inference System (E-FIS) and Human-Interaction Fuzzy Inference System (HI-FIS), respectively. In the E-FIS, the environment temperature, humidity, and brightness were used as inputs. Fig. 4 shows the membership functions of each input respectively. These linguistic variables can take the values of cold, comfortable, or hot for the temperature input; dry, comfortable and wet for humidity; and low or high for brightness. The ranges of these linguistic variables are defined based on [27] and [28]. The outputs of the E-FIS are PAD model values (Pleasure, Dominance and Arousal), which can take the values of low, neutral or high. The range of each PAD axis is from −10 to 10. Gaussian distributions are used to model the membership functions. The number of rules defined in the E-FIS is 18.

The E-FIS system uses an adaptive function, which is modified according to the robot's temperature. The output of this adaptation changes the membership functions in E-FIS generating new PAD values that produce a suitable robot motion. The main idea of this approach is to replicate, in the robot, the influence of body temperature on human thermal comfort perception [29], a physiological value that can be linked to affective states.

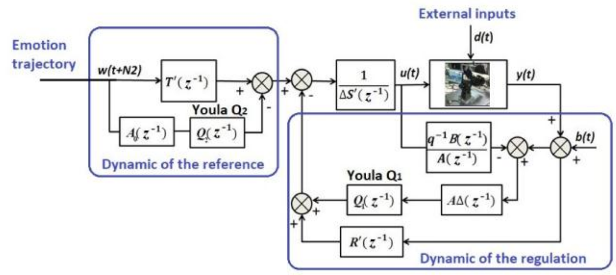

Figure 7. Robust Generalized Predictive Controller structure (RGPC)

For the HI-FIS, the input is the distance between the human and the robot. This distance is calculated by the human state component as the average of the joint distances detected by the Kinect. The linguistic values were defined in human proxemics studies [30]. This variable can take values of *personal*, *social*, and *public*, as shown in Fig. 5. As the E-FIS, the PAD values are used as HI-FIS outputs. However, for the HI-FIS, the human state inputs detected by Kinect are used to change the membership function parameters in the output variables. An example is shown in Fig. 6 for the pleasure output. This figure shows how the values of the mean of the Gaussian functions of each linguistic value are changed to positive values when a smile is detected by the perceptual system. This makes the robot's emotional state tend to be more positive when the human explicitly expresses a positive emotion. A total of three rules were used in the HI-FIS model.

The outputs of the E-FIS and HI-FIS are represented by the vector $\mathbf{PAD}_{env} = [P_{env}, A_{env}, D_{env}]^T$ and $\mathbf{PAD}_{hi} = [P_{hi}, A_{hi}, D_{hi}]^T$ respectively. The current PAD value is calculated as:

$$\begin{aligned} P_c &= \alpha P_{hi} + \beta P_{env} \\ A_c &= \alpha A_{hi} + \beta A_{env} \\ D_c &= \alpha D_{hi} + \beta D_{env} \end{aligned} \tag{2}$$

where the P_c, A_c and D_c indicate the current value of Pleasure, Arousal and Dominance, respectively. The values of α and β are parameters that can be used to personalize the influence of the human actions and environmental conditions, and they affect the robot's internal affective model. For this design, the values were set to α =1 and β =0.5.

The current value of the **PAD** vector $\mathbf{PAD}_c$ is used to classify the current affect using the K-NN (k-nearest neighbors) algorithm [31]. In the proposed approach, the K-NN algorithm is trained, assigning a vector value inside of the 3-axis PAD space to each affect. In K-NN, an unlabeled vector is classified by assigning the label which is most frequent among the k training samples nearest to that query point. Using a value of k=1, a given PAD vector input can be assigned to a class (affect) of its single nearest neighbor. For this work, only the affects shown in Fig. 1 are used to train the K-NN algorithm.

V. Adaptive Predictive Controllers

Predictive controllers are extensively developed for different industrial applications [32]. There are different kinds of predictive controllers using a reference system model (MPC). One of them is the Robust Generalized Predictive Control (RGPC), which is designed based on predictive controllers and robustified with optimization. For this work, we proposed an RGPC controller optimized by Youla parametrization (Fig. 7) to increase the robot motion performance for external perturbations and uncertainty parameters.

The adaptive robust predictive controllers for sensitive robotics are a new application, and it is one of the work's main contributions. RGPC is designed using the base of GPC controllers, and robustified by Youla parameters with convex optimization.

The affective PAD model is used to design the control optimization parameters. The PAD values influence the horizons and the weighting signal control parameter to determine the GPC optimization's cost function.

The GPC control predicts the final signal control using the robot dynamic model, a receding horizon based on minimum time events, and a reference trajectory determined according to the PAD variation and adaptive FIS controller for the robot to express emotions.

The predictive control strategy is described for the following sequence [33]: 1) definition of a model to predict the future, 2) minimization of a quadratic cost function over a finite future horizon, 3) calculation of a sequence of control values in the future, and 4) iteration of the procedure in each sampling period according to the receding horizon strategy.

The GPC controller is designed using the CARIMA model (Controlled Auto-Regressive Moving-Average) [34], which is represented by the robot dynamics and external input (signal of the environment or human interaction) in an integrated model. The CARIMA model is given by

$$A(z^{-1})y(t) = B(z^{-1})u(t-1) + \frac{C(z^{-1})}{\Delta}\xi(t) \tag{3}$$

$A(z^{-1})$and $B(z^{-1})$ are the polynomials of the dynamic robot model simplified. *u(t)* is the robot joints torque, *y(t)* is the robot position, and $\xi(t)$is the perturbation modeled as a Gaussian noise. The polynomial $C(z^{-1})$ represents external influences. Δ is a difference operator to get minimal static error. The robot model was linearized as a nominal model for RGPC design. The models are converted to discrete time with a sample time Ts = 0.01s.

By minimizing the cost function (4), the control signal is calculated. It is constituted by the optimum predictive output $\hat{y}(t+j|t)$, the future reference trajectory $w(t+j)$, and the output prediction horizons: N_1 (initial horizon), N_2 (final horizon), and N_u (horizon over the control signal).

$$J = \sum_{j=N_1}^{N_2} [(\hat{y}(t+j|t) - w(t+j)]^2 + \sum_{j=N_1}^{N_u} (\lambda(j)\Delta u^2(t+j-1)) \quad (4)$$

The optimization process is configured for each robot joint with N_1, N_2, N_u, and λ. The control parameters are designed to obtain expressive motions inside the stable criterium and response time with temporal and frequency constraints. The horizons were determined by minimum time events, occurring in a short time, to represent expressions in the robot.

The Adaptive Robust GPC is designed using adaptive variables in the optimization process. These variables are N_2 as the final horizon for the prediction and λ as the weighting parameter in the control signal. These parameters are modified according to the influence of the environment and human interaction ($\mathbf{PAD}_c$).

The final horizon for the prediction N_2 is an adaptive term in the optimization process. N_2 changes according to $\mathbf{PAD}_c$, modifying the response velocity in the final robot expression by

$$N_2 = f_1(\mathbf{PAD}_c) \quad (5)$$

The other important parameter influencing the robot's expressive response is λ, the weight on increments of the control signal. This parameter moves the controllers to get stable controllers and determines the robot oscillations; finally, it affects the robot expression. $u(t)$ and $u(t+j)$ are the control signal. $\mathbf{PAD}_c$ influences the value of the optimal λ to obtain the different final expressions of the robot (6).

$$\lambda = f_2(\mathbf{PAD}_c) \quad (6)$$

The functions f_1 and f_2 are determined as the mean value of the $\mathbf{PAD}_c$, where the maximum and minimum values represent the maximum and minimum value for N_2 that guarantee stable controllers for the robot arm. For this work, the robot horizon changes in the range N_2 = [10–200].

Equation (7) represents the signal control implemented in the robot to get the expressive motions using synthesized polynomials $R(z^{-1})$, $S(z^{-1})$ and $T(z)$. They are calculated by minimizing the quadratic criterion in the GPC optimization.

$$S(z^{-1})\Delta(z^{-1})u(t) = -R(z^{-1})y(t) + T(z)(w(t) + N_2) \quad (7)$$

The previous GPC is robustified by solving a convex optimization problem, using Youla parametrization to obtain robust predictive controllers [35], [36].

With the robot characteristic polynomial $A_0A_c = \Delta AS + z^{-1}BR$, the RGPC is calculated in a feedback compensation to determine the initial stabilizing controllers, where A_c represents the control dynamic and A_0 is for observer dynamic.

RGPC is defined by stable transfer functions as $Q = [Q_1\ Q_2]$ (8).

$$K(z^{-1}) = \left[\frac{T(z^{-1}) - A_0Q_2}{S - z^{-1}BQ_1} - \frac{R + \Delta AQ_1}{S - z^{-1}BQ_1}\right] \quad (8)$$

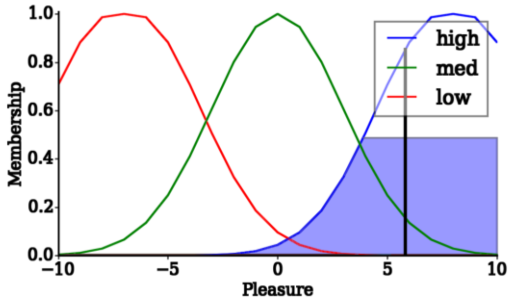

Figure 8. Defuzzification example

The RGPC structure is presented in Fig. 7, where the robot's motion trajectory is adjusted to the **PAD** mapping with Q_2 by the dynamic of the following reference, and Q_1 modifies the internal regulation dynamics. The new RGPC controller is represented by $R_Y(z^{-1})$, $S_Y(z^{-1})$, and $T_Y(z^{-1})$ as functions of Q_1, Q_2, and robot dynamics (9).

$$\begin{aligned} T_Y(z^{-1}) &= T(z^{-1}) - A_0(z^{-1})Q_2(z^{-1}) \\ R_Y(z^{-1}) &= R(z^{-1}) + \Delta(z^{-1})A(z^{-1})Q_1(z^{-1}) \\ S_Y(z^{-1}) &= S(z^{-1}) - (z^{-1})B(z^{-1})Q_1(z^{-1}) \end{aligned} \quad (9)$$

Youla parameters $Q = [Q_1\ Q_2]$ are calculated by convex optimization, applying frequency and temporal constraints, according to the expressive motions and minimum time to produce the expressions in the robot.

A. *Frequency Constraints for the Optimization*

Frequency specifications are applied to make the control response more robust, using an uncertainty model and the small gain theorem which gives stability properties in each transfer function with uncertainty [34]. To analyze the controller's stability, the Nyquist criterion is applied to the optimization. Frequency constraints are modeled by an unstructured uncertainty, where $P(z^{-1})$ is a robot model connected to Δu, an additive direct uncertainty. The robustification is maximized by minimizing the norm H_∞ in (10).

$$\min_{Q_1 \in \Re H_\infty} \|P(z^{-1})W(z^{-1})\|_\infty \quad (10)$$

$W(z^{-1})$ is a weighting transfer function with a frequency band where uncertainties due to environmental effects are considered. This specification is convex in Q_1 in a space $H\infty$ where all transfer matrices are stable.

B. *Temporal Constraints for the Optimization*

To keep external inputs within temporal restrictions, the optimization is configured using constraints inside of a temporal template $\Phi(Q)_{ijoint}$ for each robot joint with maximum amplitude = [10–20], minimum amplitude = [−5, −30], time = [2s–5s], and order of Youla parameters = [5–50]. This order allows linear parametrization over each of the robot model's transfer functions.

The solution of $\Phi(Q)_{ijt}$ is obtained by linear programming using convex optimization. The optimization minimizes the H_∞ norm with constraints by a temporal template. $\Phi(Q_{1ijt})$ is a temporal template to manage external effects (environment or human activity), and $\Phi(Q_{2ijt})$ is a template to reject measurement noise (11)

$$\begin{gathered}\min_{Q_1\in\Re H_\infty}\left\|\left(\frac{-RA-A^2\Delta u Q_{1ijt}}{A_0A_c}\right)W(z^{-1})\right\|_\infty \\ \min_{Q_2\in\Re H_\infty}\left\|\left(\frac{-TA-A^2A_0 Q_{2ijt}}{A_0A_c}\right)W(z^{-1})\right\|_\infty\end{gathered} \tag{11}$$

Applying Q_1, minimization of H_∞ norm, and temporal constraints is solved the convex optimization.

VI. Simulated Results

A. Adaptive Fuzzy Logic Controller

This section shows the proposed adaptive fuzzy logic controller's performance in modeling emotional states. Fig. 8 presents a defuzzification example acting in the Pleasure output with the adaptive input. Figs. 9, 10, and 11 show how the Pleasure, Dominance and Arousal values produced by the HI-FIS change in function of the distance of the human approaching the robot.

When no facial expressions are detected, the **PAD** value remains at 0 until the human approaches the robot's social space, which increases the pleasure and arousal values. It produces the **PAD** vector to stay closer to a surprised emotional action. When a smile is detected, the three **PAD** values are increased, producing a closer tendency to a *"Happy"* affect. When the human ignores the robot with the gaze, the **PAD** values are adapted to get closer to the "*Sad*" affect.

Fig. 12 represents the robot's adaptive response to environmental variations and changes in the robot **PAD**. The red circles in this figure represents the most significant changes in the surfaces of each **PAD** output, and the adaptive response to the temperature and humidity variation.

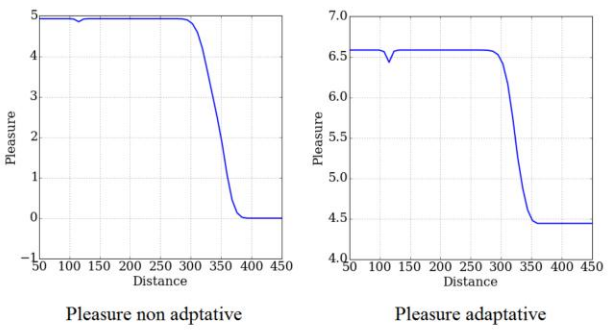

Figure 9. Pleasure output of the HI-FIS with the influence of a positive adaptive input

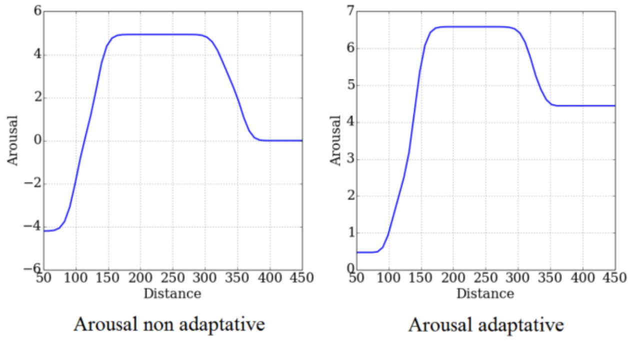

Figure 10. Arousal output of the HI-FIS with the influence of a positive adaptive input

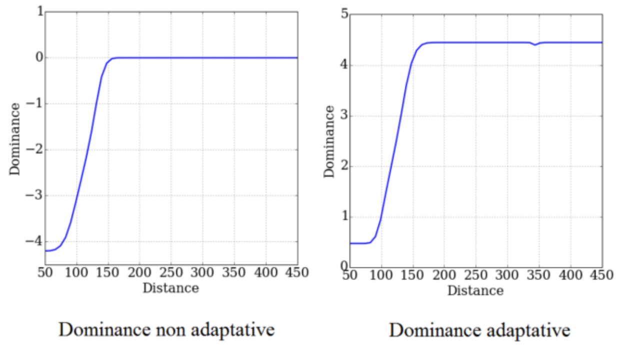

Figure 11. Dominance output of the HI-FIS with the influence of a positive adaptive input

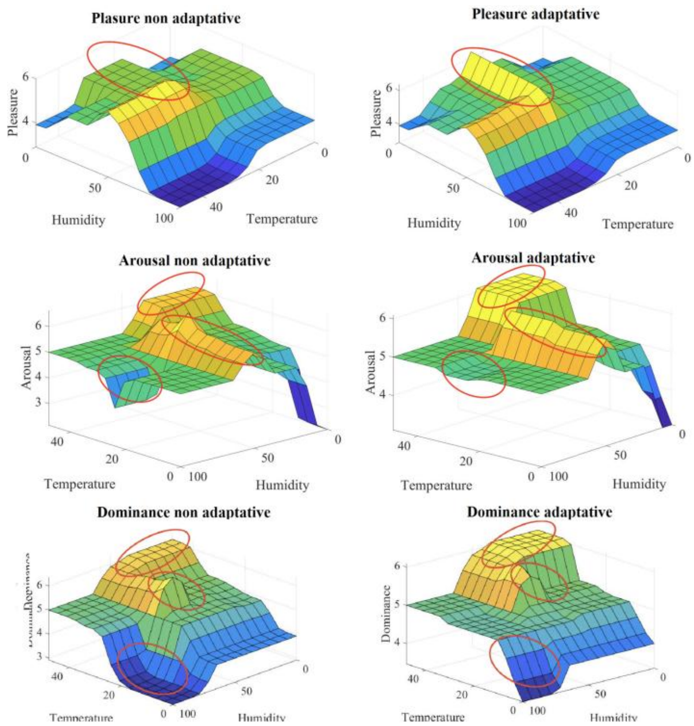

Figure 12. **PAD** in the robot motion with the influence of the adaptive controllers

B. Adaptive Robust Predictive Controllers

The GPC controllers are designed with the parameters shown in Table I by each robot joint with an initial horizon N_1=1 and control signal limit N_u=1. The values on this table represent an example of the GPC design control for a low and high **PAD**$_c$ that produce a "*Happy*" state in the robot. N_{2a} represents a **PAD**$_c$ with high Arousal, N_{2b} medium **PAD**$_c$, and N_{2c} low Arousal in the **PAD**$_c$. In the horizons of prediction design, the values of Arousal that represent the velocity in robot states are taken into account. The initial horizon for the optimization N_2 and the optimal λ_1 change according to the adaptability of the **PAD**$_c$ values.

TABLE I: GPC PARAMETERS FOR ROBOT STATES WITH **PAD**$_c$ EFFECT

Joints	N_{2a}	λ_1	N_{2b}	λ_2	N_{2c}	λ_3
J_1	20	0.33	70	42.7	120	124.7
J_2	25	0.25	75	28.28	125	127.7
J_3	11	2.02	61	65.52	111	114.5
J_4	9	10.41	59	60.58	109	110.58
J_5	10	11.8	60	61.78	110	111.78

Figs. 13 and 14 show the GPC stability and robustness responses in a Black and Bode diagrams for the base of initial horizon N_{2a} for high **PAD**$_c$ and more Arousal value in the robot state. Table II shows the results of GPC stability in terms of the Margin of Gain (MG), Margin of Phase (MP), and Margin of delay (MD). The results present an incremental MG and MP when the **PAD** influence is reduced, indicating that the distance is large (human far from the robot, in a public zone), and it produces a low velocity in the robot motion.

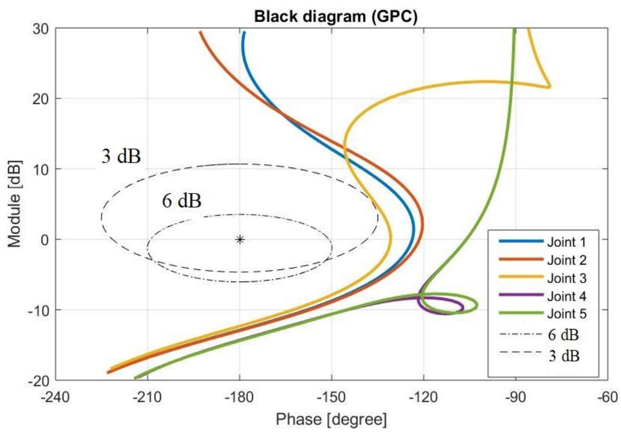

Figure 13. GPC responses (Black diagram) Robustness and sensibility for a high **PAD**

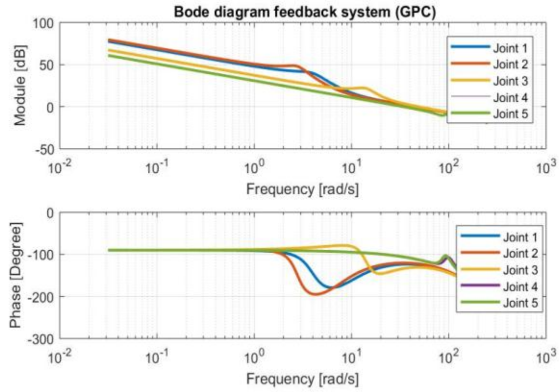

Figure 14. GPC responses (Bode diagram) frequency response for a high **PAD**

TABLE II: GPC VALUES OF THE STABILITY

	N_{2a} and λ_1			N_{2c} and λ_3		
Joints	MG [*dB*]	MP [*degree*]	MD [*ms*]	MG [*dB*]	MP [*degree*]	MD [*ms*]
J_1	12.9	56.3	2.21	14.02	70.89	3.1
J_2	13	58.0	2.3	13.9	70.3	3.04
J_3	12.83	48.7	1.8	14.5	71.4	3.24
J_4	14.29	73.9	3.7	14.44	72.03	3.16
J_5	14.33	73.98	3.8	14.41	72.03	3.17

Figs. 15 and 16 show the GPC controller's different responses (Black and Bode diagrams). When the **PAD** decreases the values, N_2 is incremented, and it affects the complementary and direct robot sensibility (data circle in 3 dB and 6 dB in the Black diagram). The robot shows a low velocity with the same emotion "*Happy*," keeping a stable motion and producing a response more distributed for all joints (Fig. 15).

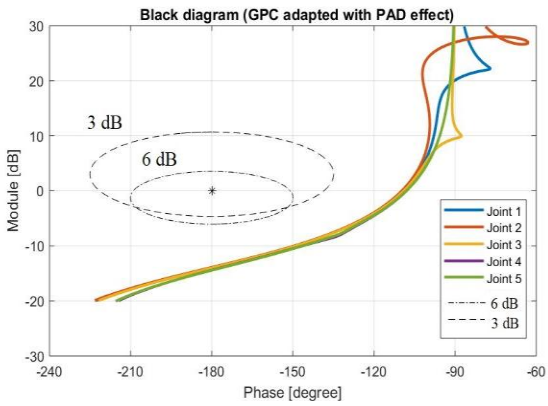

Figure 15. GPC responses (Black diagram) Robustness and sensibility for a low **PAD**

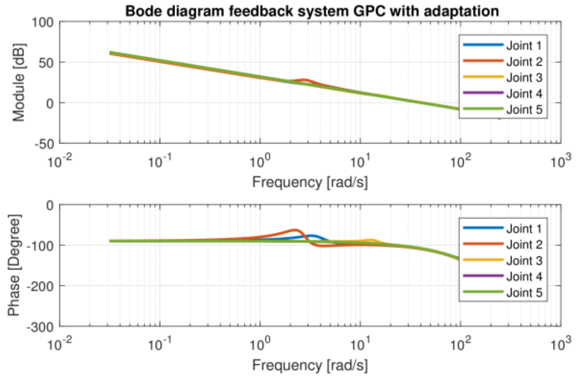

Figure 16. GPC responses (Bode diagram) Frequency responses for a low **PAD**

The Robust GPC is designed using the base of the GPC controllers (Table I), and is updated according to the **PAD**$_c$ values. Table III shows the parameters used to design and optimize the RGPC.

TABLE III: RGPC DESIGN PARAMETERS

Param.	J_1	J_2	J_3	J_4	J_5
Max. TI	20	30	30	10	10
Min TI	−5	−10	−10	−10	−10
T_r time	5s	2s	2s	2s	2s
$W(z^{-1})$	$\frac{[1,-0.6]}{0.3}$	$\frac{[1,-0.8]}{0.5}$	$\frac{[1,-0.8]}{0.5}$	$\frac{[1,-0.7]}{0.5}$	$\frac{[1,-0.7]}{0.5}$
Order ***Q***	50	10	15	5	5

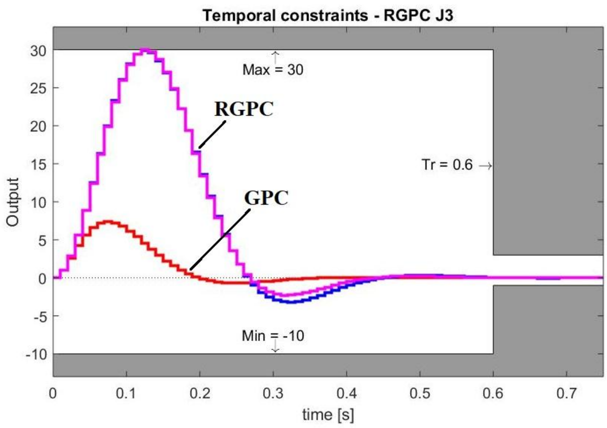

Figure 17. Robust GPC for the robot motion

Fig. 17. shows the robustification of the controllers RGPC. This response represents the initial GPC controllers with a temporal template, which is used as constraints in the optimization by Youla parametrization.

The stability and robustness results for the robot using RGPC with a high **PAD** are presented in Figs. 18 and 19. These figures show that the controllers act with stability, and the high **PAD**'s influence produces different direct sensibility in all robot joints. This response is more pronounced when the **PAD** values decrease (Figs. 20 and 21) in joint 1, 2 and 3.

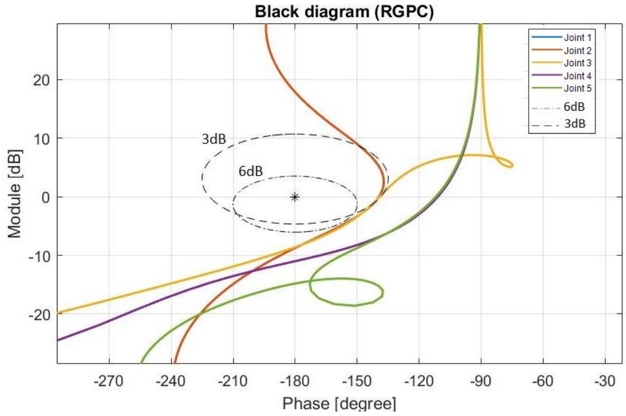

Figure 18. RGPC Black diagram for a high **PAD**

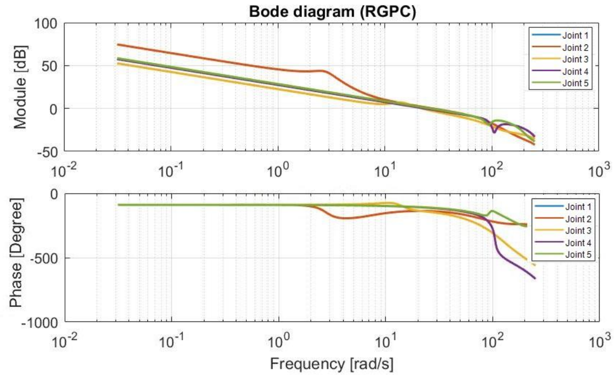

Figure 19. RGPC Bode responses for a high **PAD**

The final effect is represented directly with the velocity and smooth effect during the real robot motion, as shown by the errors explained in section VII (Experimental section). The temporal constraints for the optimization in the RGPC with the effect of the **PAD** are showed in Table IV.

TABLE IV: RGPC PARAMETERS WITH **PAD** EFFECT

Param.	J_1	J_2	J_3	J_4	J_5
Max. TI	60	100	20	10	10
Min TI	−15	−30	−10	−10	−10
Tr time	2.5s	3s	2s	1s	1s
$W(z^{-1})$	$\frac{[1,-0.6]}{0.3}$	$\frac{[1,-0.8]}{0.5}$	$\frac{[1,-0.8]}{0.5}$	$\frac{[1,-0.7]}{0.5}$	$\frac{[1,-0.7]}{0.5}$
Order ***Q***	50	10	15	5	5

VII. EXPERIMENTAL RESULTS AND VALIDATION

The robot platform, explained previously, was used as the experimental setup. Three types of experiments were conducted, focusing on variations in environmental parameters, human interaction, and robot temperature to validate the control architecture and expressive robot motions.

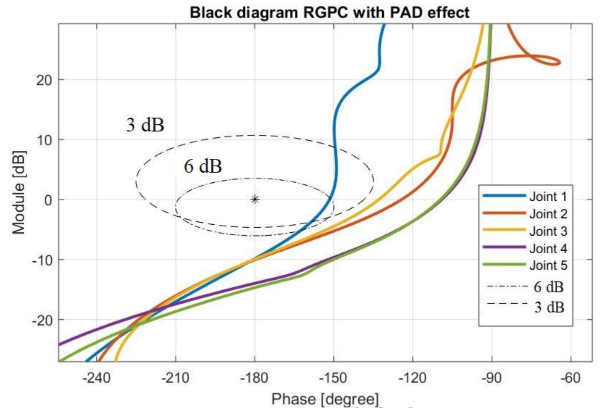

Figure 20. RGPC Black diagram for a low **PAD**

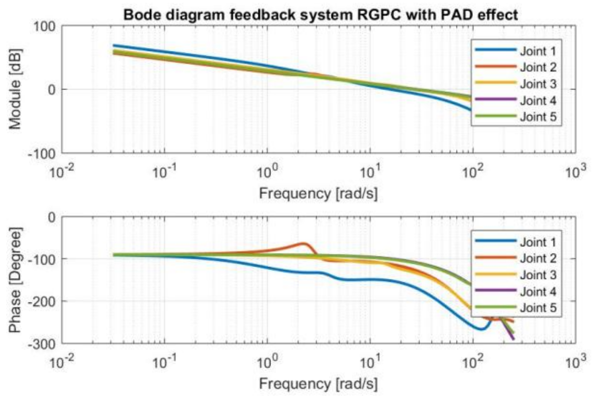

Figure 21. RGPC Bode diagram for a low **PAD**

A. Variation of Environment Parameters

In this experiment, the environmental parameters (temperature (T), humidity (H) and brightness (B)) are changed. A human in a public space distance was presented for this experiment. As mentioned in section VI, human presence will not affect the **PAD** value until human approaches the social space. The values of P_{hi}, A_{hi}, D_{hi} are therefore zero.

Robot motions generated by the **PAD** were chosen to represent four extreme affective motions: *"Happy"*, *"Sad"*, *"Angry"* and "*Protected"*. Table V shows the results of the robot **PAD** and response to each emotion with the control RMSE error.

The *"Happy"* motion is expressed by the robot when the comfort values of temperature and humidity, together with enough brightness, are presented. The *"Sad"* motion is expressed when the environment temperature decreases to cold values and there is not enough brightness in the environment. The robot expresses *"Angry"* motions when the temperature reaches high values and low humidity with enough brightness.

Finally, "*Protected"* motions are expressed in high temperatures, humidity, and low brightness.

The *"Happy"* motion presented a high **PAD** robot values compared to the other motions and higher values in the control error. In this case, the velocity was increased, and it modified the mapping to produce the robot motions.

B. Variation of Human Distance

In this experiment, we want to detect the effect on the robot's affective states when a human is approaching the robot's social space. The environment is set to get the *"Happy"* emotion. The human distance varied in values of 402 cm, 350 cm and 180 cm, and generated the motion *"Happy 1"*, *"Happy 2"*, and *"Happy 3"* . In Table VII, it is shown how the HI-FIS has a larger influence on the robot's emotional state for the pleasure and arousal components when the human gets closer to the robot. The results showed how the velocity varies, producing the same emotion *"Happy"*. It shows the control adaptation with predictive controllers, when the $\mathbf{PAD}_c$ changes the control parameters, and they are adapted, modifying the velocity according to the variation in the predictive horizon parameter.

C. Variation of Robot Temperature

This experiment was developed by moving the robot to get the joints temperature. To avoid damage to the system, this experiment was set to extreme values in the robot with minimum and maximum temperatures (exceeded 34℃). The robot temperature affects the adaptive FIS controller (AFEM) and modifies the **PAD** values. The control performance and robot motion were evaluated and are shown in Table VII.

To detect variation in the robot states when the robot temperature changes, experiments were conducted using low and high robot temperature values. The values applied for the experiments were 10 and 40 ℃. The other perceptual inputs were set to fixed values, and only the robot temperature was changed. The robot temperature modifies the input in the adaptive FIS controller (Fig. 3). This input affects the standard deviation of the membership function in the E-FIS (Environment FIS). During the experiments, the human distance was set to a public zone value (405 cm) (Fig. 5), which has less impact on the final $\mathbf{PAD}_c$ caused by human interaction, and it allows more action of the robot temperature effect.

From the robot sensors, the joints temperatures are sent for the perceptual module; this module takes the average value of the temperatures of all joints. Table II shows the experimental results. The output showed that the final $\mathbf{PAD}_c$ has negative values for a low robot temperature producing a low pleasure, arousal and dominance, and they represent a robot motion with a *"Sad"* state. In the other case, with a high temperature, the **PAD** had positive value in pleasure, and negative values in arousal and dominance. The robot with the high temperature represented a low pleasure state, with a result of "*Protected"* motion that also corresponded to the state to avoid damage inside of the robot system. This state causes less robot motion in terms of velocity compared to other states, such as *"Happy"*, and because of lower velocity and motion, the robot can balance the temperature in all joints, maintaining a safe state waiting for other motions.

Fig. 22 shows the results of the robot in different expressive motions after executing the adaptive controllers HI-FIS, E-FIS and RGPC. This result shows how the robot responds to different states according to the perceptual inputs (human interaction, environment and robot measurement), cognitive processes, and adaptive controllers. In this figure, the different robot motions are showed as resulted of the adaptive control system. These

TABLE V: RESULTS FOR VARIATIONS IN THE ENVIRONMENT PARAMETERS

Perceptual Inputs				Output of FIS and RGPC controllers										
Ds (cm)	*T* (℃)	*H* (%)	*B* (%)	P_{env}	A_{env}	D_{env}	P_{hi}	A_{hi}	D_{hi}	P_c	A_c	D_c	RMSE (rad)	Robot state
402	25	50	70	5.8	5.4	5.8	0.0	0.0	0.0	5.8	5.4	5.8	0.46	*Happy*
408	5	80	10	−2.2	−3.5	−2.7	0.0	0.0	0.0	−2.2	−3.5	−2.7	0.23	*Sad*
405	40	10	70	−4.2	5.49	5.43	0.0	0.0	0.0	−4.2	5.49	5.43	0.98	*Angry*
402	38	78	10	5.6	−3.5	−2.7	0.0	0.0	0.0	5.6	−3.5	−2.7	1.7	*Protected*

TABLE VI: RESULTS FOR VARIATIONS IN THE HUMAN DISTANCE

Perceptual Inputs				Output of FIS and RGPC controllers											
Ds (cm)	*T* (℃)	*H* (%)	*B* (%)	P_{env}	A_{env}	D_{env}	P_{hi}	A_{hi}	D_{hi}	P_c	A_c	D_c	RMSE (rad)	Velocity (RMS)	Robot state
402	25	50	70	5.8	5.4	5.8	0.0	0.0	0.0	5.8	5.4	5.8	0.46	0.51	*Happy 1*
350	25	50	70	5.8	5.4	5.8	2.0	2.0	0.0	6.8	6.4	5.8	0.53	0.59	*Happy 2*
180	25	50	70	5.8	5.4	5.8	4.9	4.9	0.0	8.2	7.95	5.8	0.59	0.64	*Happy3*

TABLE VII: RESULTS FOR VARIATIONS IN THE ROBOT TEMPERATURE

Perceptual Inputs					Output of FIS and RGPC controllers										
Ds (cm)	*T* (℃)	T_{robot} (℃)	*H* (%)	*B* (%)	P_{env}	A_{env}	D_{env}	P_{hi}	A_{hi}	D_{hi}	P_c	A_c	D_c	RMSE (rad)	Robot state
405	8	10	80	10	−3.7	−5.2	−2.7	0.0	0.0	0.0	−3.7	−5.2	−2.7	0.13	*Sad*
405	8	40	80	10	1.7	−5.3	−2.7	0.0	0.0	0.0	1.7	−5.3	−2.7	0.19	*Protected*

final expressions change with trajectories involving the robot's dynamic information in position and velocity. The robot's states are produced with a variation in robot's parameters to give a different sensation when the robot's adaptive system is activated. In this result, the variation produced in the end-effector is shown, which modified the robot expression significantly, as well as the other robot joints position that express the final state. The adaptive controllers allowed to generate robot motions with personalized interaction between human, environmental, and robot states. Experimental video of this work showing the expressive robot motion during the human and environmental interaction can be visualized in the link (1).

VIII. CONCLUSIONS

In this paper, a novel adaptive control architecture for simulation and expression of emotional states in a robot arm was developed, determined by perception, cognition and emotion expression levels. The adaptive system generates **PAD** values for the robot motion according to the environmental, human interaction, and robot current states.

(1) https://youtu.be/q1DO4PBSA6M

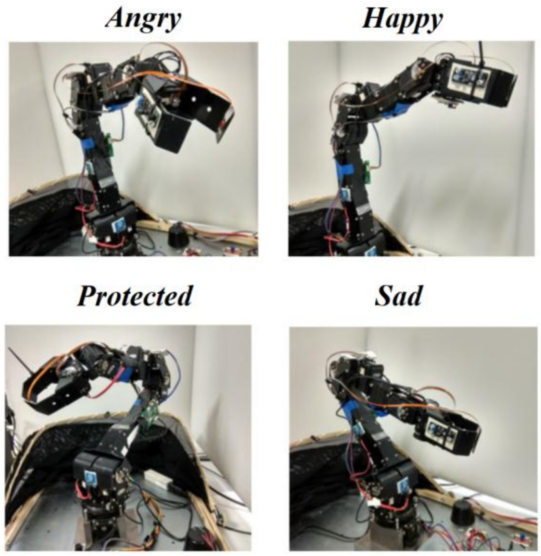

Figure 22. Expressive robot motions in the real robotic platform

The control architecture is based on adaptive fuzzy System and Robust Predictive controllers by optimization with Youla parameters. The affective model PAD was used to determine perception inputs from the human and environment. The human interaction directly affected the **PAD** values and, therefore, the robot's response via the adaptive controllers produces motion states with different positions and velocities. With this result, the robot is able to engage with humans in different degrees of motion with the same expression or move for other expressive motions if the environment or robot parameters are modified by the perception level. It indicates that the robot can conduct state expressions in a wide range of possibilities, according to perceptual inputs, cognitive processes, and adaptive controllers. Also, the effects of the adaptive cognitive system by fuzzy algorithms and predictive controllers influence the result based on the affective PAD model, producing different kinds of motions. The adaptive parameters in the predictive control influence the motion velocity and change the robot's final posture.

Results showed a suitable performance of the adaptive control with variation in the PAD model to represent expressive robot states. The proposal allowed us to generate motions with more personalized characteristics in the robot to facilitate a better interaction between robots, humans, and the environment. Due to the developed architecture's modular design, it can be easily adapted to other types of robots and sensors. Future work will be oriented toward applying the proposed adaptive controllers to multi-robot-multi-human environments.

ACKNOWLEDGMENT

This research is supported by the JSPS Grant in Aid for challenging exploratory research K115K12124 and the Bilateral program JSPS-DST 7270525301.

REFERENCES

[1] G. Lakatos, M. Gacsi, V. Konok, I. Brúder, B. Bereczky, P. Korondi, and Á. Miklósi, "Emotion attribution to a non-humanoid robot in different ´ social situations," *PloS One*, vol. 9, no. 12, p. e114207, 2014.

[2] M. Dubois, J. A. Claret, L. Basanez, and G. Venture, "Influence of emotional motions in human-robot interactions," in *Int. Symp. on Experimental Robotics*. Springer, 2016, pp. 799–808.

[3] A. Mehrabian and S. R. Ferris, "Inference of attitudes from nonverbal communication in two channels." *J. of consulting psychology*, vol. 31, no. 3, p. 248, 1967.

[4] C. Breazeal, "Emotion and sociable humanoid robots," *Int. J. of Human Computer Studies*, vol. 59, no. 1, pp. 119–155, 2003.

[5] D. Mazzei, N. Lazzeri, D. Hanson, and D. De Rossi, "Hefes: A hybrid engine for facial expressions synthesis to control human-like androids and avatars," in *Biomedical Robotics and Biomechatronics (BioRob), 2012 4th IEEE RAS & EMBS Int. Conf. on. IEEE*, 2012, pp. 195–200.

[6] J. Novikova and L. Watts, "A design model of emotional body expressions in non-humanoid robots," in *Proc. the Second Int. Conf. on Human-agent Interaction*. ACM, 2014, pp. 353–360.

[7] J. M. Angel-Fernandez and A. Bonarini, "Robots showing emotions," *Interaction Studies,* vol. 17, no. 3, pp. 408–437, 2017.

[8] J. Zhang, J. Zheng, and N. Magnenat-Thalmann, "Modeling personality, mood, and emotions," in *Context Aware Human-Robot and Human Agent Interaction*. Springer, 2016, pp. 211–236.

[9] J. A. Russell and A. Mehrabian, "Evidence for a three-factor theory of emotions," *Journal of research in Personality*, vol. 11, no. 3, pp. 273–294, 1977.

[10] M. Karg, A. A. Samadani, R. Gorbet, K. Kuhnlenz, J. Hoey, and D. Kulic, "Body movements for affective expression: A survey of automatic recognition and generation," *IEEE Transactions on Affective Computing*, vol. 4, no. 4, pp. 341–359, 2013.

[11] M. M. Bradley and P. J. Lang, "Measuring emotion: the self-assessment manikin and the semantic differential," *J. of behavior therapy and experimental psychiatry*, vol. 25, no. 1, pp. 49–59, 1994.

[12] L. Pena, J. M. P. Sanchez, and S. Ossowski, "Representing emotion and mood states for virtual agents." in *MATES*. Springer, 2011, pp. 181–188.

[13] A. Popescu, J. Broekens, and M. Van Someren, "Gamygdala: An emotion engine for games," *IEEE Trans. on Affective Computing*, vol. 5, no. 1, pp. 32–44, 2014.

[14] J. A. Claret, G. Venture, and L. Basanez, "Exploiting the robot kinematic ˜ redundancy for emotion conveyance to humans as a lower priority task," *Int. J. of social robotics*, vol. 9, no. 2, pp. 277–292, 2017.

[15] A. Nanty and R. Gelin, "Fuzzy controlled pad emotional state of a nao robot," in *Technologies and Applications of Artificial Intelligence (TAAI), 2013 Conf. on. IEEE*, 2013, pp. 90–96.

[16] S. A. Ajwad, J. Iqbal, M. I. Ullah, and A. Mehmood, "A systematic review of current and emergent manipulator control approaches," *Frontiers of Mechanical Engineering*, vol. 10, no. 2, pp. 198–210, 2015.

[17] F. Liao, Y. Xu, and J. Wu, "Novel approach to preview control for a class of continuous-time systems," *Journal of Control Science and Engineering*, vol. 2015, p. 10, 2015.

[18] A. P. Aguiar, J. P. Hespanha, and P. V. Kokotovic, "Performance limitations in reference tracking and path following for nonlinear systems," *Automatica,* vol. 44, no. 3, pp. 598–610, 2008.

[19] B. Olofsson and L. Nielsen, "Path-tracking velocity control for robot manipulators with actuator constraints," *Mechatronics*, vol. 45, pp. 82–99, 2017.

[20] I. Eliasson, I. Knez, U. Westerberg, S. Thorsson, and F. Lindberg, "Climate and behaviour in a nordic city," *Landscape and Urban Planning*, vol. 82, no. 1, pp. 72–84, 2007.

[21] M. E. Segura, E. Coronado, M. Maya, A. Cardenas, and D. Piovesan, "Analysis of recoverable falls via microsoft kinect: Identification of third-order ankle dynamics," *J. of Dynamic Systems, Measurement, and Control*, vol. 138, no. 9, p. 091006, 2016.

[22] D. C. Schmidt, M. Stal, H. Rohnert, and F. Buschmann, Pattern-Oriented Software Architecture, *Patterns for Concurrent and Networked Objects*. John Wiley & Sons, 2013, vol. 2.

[23] E. Coronado, F. Mastrogiovanni, and G. Venture, "Design of a Human-Centered Robot Framework for End-User Programming and Applications." In ROMANSY 22-Robot Design, Dynamics and Control. vol 584. Springer, Cham, 2018.

[24] M. Quigley, K. Conley, B. Gerkey, J. Faust, T. Foote, J. Leibs, R. Wheeler, and A. Y. Ng, "Ros: an open-source robot operating system," in *ICRA Workshop on Open Source Software*, vol. 3, no. 3.2. Kobe, 2009, p. 5.

[25] T. Katsumata, et al., "Dynamics identification and control during a contact painting task without external sensors," *IEEE Trans. in Robotics*, 2017.

[26] A. Van Der Heide, D. Sanchez, and G. Trivino, "Computational models ´ of affect and fuzzy logic," in *Proc. the 7th Conference of the European Society for Fuzzy Logic and Technology*. Atlantis Press, 2011, pp. 620–627.

[27] J. J. Pilcher, E. Nadler, and C. Busch, "Effects of hot and cold temperature exposure on performance: a meta-analytic review," *Ergonomics*, vol. 45, no. 10, pp. 682–698, 2002.

[28] W. Fincher and M. Boduch, "Standards of human comfort: relative and absolute," 2009.

[29] C. J. Willemse, D. K. Heylen, and J. B. van Erp, "Warmth in affective mediated interaction: Exploring the effects of physical warmth on interpersonal warmth," in *Affective Computing and Intelligent Interaction* (ACII), 2015 Int. Conf. on. IEEE, 2015, pp. 28–34.

[30] J. C. Baxter, "Interpersonal spacing in natural settings," *Sociometry*, pp. 444–456, 1970.

[31] N. S. Altman, "An introduction to kernel and nearest-neighbor nonparametric regression," *The American Statistician*, vol. 46, no. 3, pp. 175–185, 1992.

[32] A. Ramdani and S. Grouni, "Dynamic matrix control and generalized predictive control, comparison study with IMC-PID," *Int. J. of Hydrogen Energy*, vol. 42, no. 28, pp 17561–17570, 2017.

[33] E. F. Camacho and C. B. Alba, Model predictive control. New Haven: Springer Science & Business Media, 2013.

[34] P. Rodriguez Ayerbe, "Robustification de lois de commande predictive par la parametrisation de youla," Ph.D. dissertation, Paris 11, Orsay, 2003.

[35] X. Qi, M. V. Salapaka, P. G. Voulgaris, and M. Khammash, "Structured optimal and robust control with multiple criteria: A convex solution," *IEEE Trans. on Automatic Control*, vol. 49, no. 10, pp. 1623–1640, 2004.
[36] P. Rodriguez and D. Dumur, "Generalized predictive control robustification under frequency and time-domain constraints," *IEEE Trans. on Control Systems Technology*, vol. 13, no. 4, pp. 577–587, 2005

Liz Rincon Ardila is an Assistant Professor at the Tokyo University of Agriculture and Technology in the Department of Mechanical Systems Engineering, GVLab. She conducts research in deep optimal and adaptive cognitive control systems for personalized Human Robot Interaction, with interests in Advanced Control, Robotics, Machine Learning and Artificial Intelligence. She worked as a postdoctoral researcher on biotechnology and nanotechnology projects at the Institute for Technological Research of Sao Paulo, Brazil, at the Center of Bio Nano Manufacturing (2013–2015). In 2013, she obtained her Ph.D. in Mechanical Engineering from the University of Campinas, UNICAMP, Brazil and L'Ecole Supérieure d'électricité, SUPELEC, France, researching in the Dynamic Behavior of CNC machine tools with emphasis in Control Architecture and optimal control strategies. In 2008, she received her M.S. in Electronic and Computer Engineering from the University of the Andes with her research in Control Education: Theory, Practice, and learning evaluation, and her bachelor in Electronic Engineering in 2003.

Enrique Coronado has completed an Engineering degree from the Autonomous University of San Luis Potosi (Mexico) in 2012 in Mechatronics Engineering. In 2017, he obtained a MSc from the Ecole Centrale of Nantes (France) and the University of Genova (Italy) in Advanced Robotics. In 2017, he became a PhD. student at the Tokyo University of Agriculture and Technology (Japan). His main research interests include: Human-Robot/Computer-Interaction, Robot Programming, Distributed Systems, Software Architectures, and Machine Learning.

Hansen Hendra is a student at the Bandung Institute of Technology (Indonesia); he was a visiting student at the Tokyo University of Agriculture and Technology (Japan).

Julyando Phan is a student at the Bandung Institute of Technology (Indonesia); he was a visiting student in the Tokyo University of Agriculture and Technology (Japan).

Zur Izzati Binti Zainalkefli is a student at the Tokyo University of Agriculture and Technology (Japan). She works on control of robots for expressive motions using Adaptive Neuro Fuzzy controllers (ANFIS).

Gentiane Venture has completed an Engineering degree from the Ecole Centrale of Nantes (France) in 2000 in Robotics and Automation and a MSc from the University of Nantes (France) in Robotics. In 2003, she obtained her PhD from the University of Nantes (France). In 2004, she joined the French Nuclear Agency (Paris, France), to work on the control of a tele-operated micro-manipulator. Later in 2004, she joined Prof. Yoshihiko Nakamura's Lab at the University of Tokyo (Japan) with the support of the JSPS. In 2006, still under Prof. Nakamura, she joined the IRT project as a Project Assistant Professor. In March 2009, she became an Associate Professor and started her own lab at the Tokyo University of Agriculture and Technology (Japan). Her main research interests include: Non-verbal communication, Human behavior understanding from motion, Human body modeling, Dynamics identification, Control of robot for human/robot interaction, Human affect recognition.